Growth and characterization of GaAs/Al/GaAs heterostructures

P. Bhattacharya, J. E. Oh, J. Singh, and D. Biswas
Department of Electrical Engineering and Computer Science, The University of Michigan, Ann Arbor, Michigan 48109-2122

R. Clarke, W. Dos Passos, R. Merlin, and N. Mestres
Department of Physics, The University of Michigan, Ann Arbor, Michigan 48109-1120

K. H. Chang and R. Gibala
Department of Materials Science and Engineering, The University of Michigan, Ann Arbor, Michigan 48109-2136

(Received 25 September 1989; accepted for publication 3 January 1990)

Theoretical and experimental aspects of the growth of GaAs/Al/GaAs heterostructures have been investigated. In these heterostructures the GaAs on top of the buried metal layer is grown by migration-enhanced epitaxy (MEE) at low temperatures (200 and 400 °C) to provide a kinetic barrier to the outdiffusion of Al during superlayer growth. The crystallinity and orientation of the Al film itself deposited on (100) GaAs at ~0 °C was studied by transmission electron diffraction, dark-field imaging, and x-ray diffraction measurements. It is found that the Al growth is polycrystalline with a grain size ~60 Å and the preferred growth orientation is (111), which may be textured in plane but oriented out of plane. The quality of the GaAs superlayer grown on top of Al by MEE is very sensitive to the growth temperature. The layer grown at 400 °C has good structural and optical quality, but is accompanied by considerable outdiffusion of Al at the Al-GaAs heterointerface. At 200 °C, where the interface has good structural integrity, the superlayer exhibits twinning and no luminescence is observed.

I. INTRODUCTION

The possibility of epitaxially growing buried metal films of low resistance and free of pin holes will allow the realization of electronic devices such as metal-base transistors. Such layers would also be important for buried ground planes and interconnects, and for realizing internal reflection planes in optoelectronic devices. There are, however, stringent requirements for such heteroepitaxy. First, single-crystal growth of the metal film is desirable. Second, the semiconductor superlayer should be epitaxial and have device-quality electrical and optical properties. Third, for single heterostructures or multilayers, it is important that the interfaces are atomically abrupt and the semiconductor superlayer is of high quality. The difficulty in realizing these stem from the usual large difference in lattice constants between metal and semiconductors, difference in preferred growth temperatures, difference in growth modes, and last, but not the least, interdiffusion and/or oxidation problems. Finally, the ability to control dislocation generation and propagation is also a key factor in the success of such heteroepitaxy.

In spite of the problems mentioned above, impressive progress has been made in the growth of these heterostructures, particularly due to the excellent work of Sands *et al.*[1-3] on intermetallic and metal-semiconductor phase transitions. Structurally well-defined GaAs-NiAl-GaAs layers have been grown by Harbison *et al.*,[4] in which Ni plays the role of preventing Al outdiffusion during superlayer growth and also acts as a template for this layer. We describe here our studies on the growth of GaAs/Al/GaAs heterostructures without the use of Ni. The theoretical issues in such heteroepitaxy, based on surface kinetics, are discussed. In particular, the superlayers of GaAs were grown by migration-enhanced epitaxy (MEE)[5,6] and have been characterized by several *in situ* and *ex situ* characterization techniques. These include reflection high-energy electron diffraction (RHEED), transmission electron microscopy (TEM), x-ray diffraction, Raman spectroscopy, photoluminescence, and secondary-ion mass spectrometry (SIMS).

II. THEORETICAL ASPECTS OF GROWTH

The semiconductor-metal-semiconductor growth sequence is a complicated process which is not well understood at present. Nevertheless, the individual growth processes are somewhat better understood, and in this section we will try to develop a conceptual understanding of these. There are two aspects to such heterostructure growth: The first is controlled by the kinetics, which in turn are controlled by the growth parameters. The second important aspect is the growth mode and orientation.

A. Compound semiconductor growth

The conceptual picture of the MBE growth process for GaAs is outlined in Fig. 1. The incorporation process for the cation (Ga) and anion (As) is quite different as shown. The difference arises since the cation impinges in an atomic form, while the anion impinges in the molecular form. Since atoms and molecules impinge randomly on the surface, the growth surface will become very rough unless (i) atoms incorporated at nonkink sites (non-step-edge sites) evaporate, or (ii) atoms at nonkink sites rapidly migrate to the kink sites. The latter is known to occur in

 © 1990 American Institute of Physics

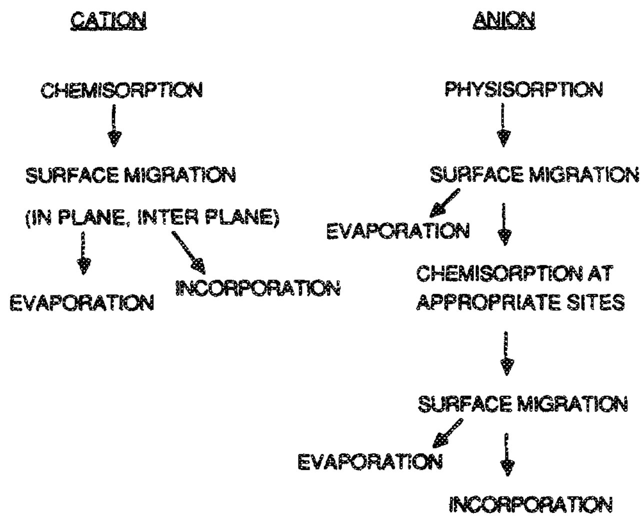

FIG. 1. Conceptual picture of MBE growth of GaAs.

GaAs MBE growth. The migration rates of cations is of more significance since, as shown in Fig. 1, the anion initially forms a weak physisorbed bonded state which can move rapidly on the surface.

Normal MBE growth is carried out under anion-rich conditions for reasons which will be explained shortly, and under these conditions the important cation migration rates are shown in Fig. 2. These rates are activated and involve breaking a Ga—As bond. The growth temperature then has to be such that this activation barrier can be overcome easily. This temperature is $\sim 550\,^{\circ}\mathrm{C}$ for GaAs growth. It is important to mention here that during the metal growth phase, the activation barrier for surface migration is controlled by the metal-metal bond strength (e.g., Al—Al) which is a much smaller energy compared to the Ga—As or Al—As bond energy. Thus the growth temperature for metal growth is very low. To reduce this temperature incompatibility between the metal and semiconductor growth, we have exploited the migration-enhanced epitaxy[5] concept.

In migration-enhanced epitaxy one moves away from the normally employed conditions of growth, i.e., use of anion overpressure. If one grows under cation overpressure, then the migration process will involve breaking a cation-cation bond (on an average), which is about half the strength of the cation-anion bond. Thus the growth temperature could be reduced by half without affecting the migration rates. However, there is a serious problem in this approach. While the excess anions do not get incorporated in the crystal, the excess cations will be incorporated, leading to a high defect density in the crystal. This can be avoided by depositing only a monolayer or so of cations in absence of the anion and then allowing the anions to impinge. Thus the cation growth occurs under cation-rich conditions and no excess cations are left. The importance of this growth procedure is that it allows the semiconductor and the metal layers to both grow under near-ideal conditions.

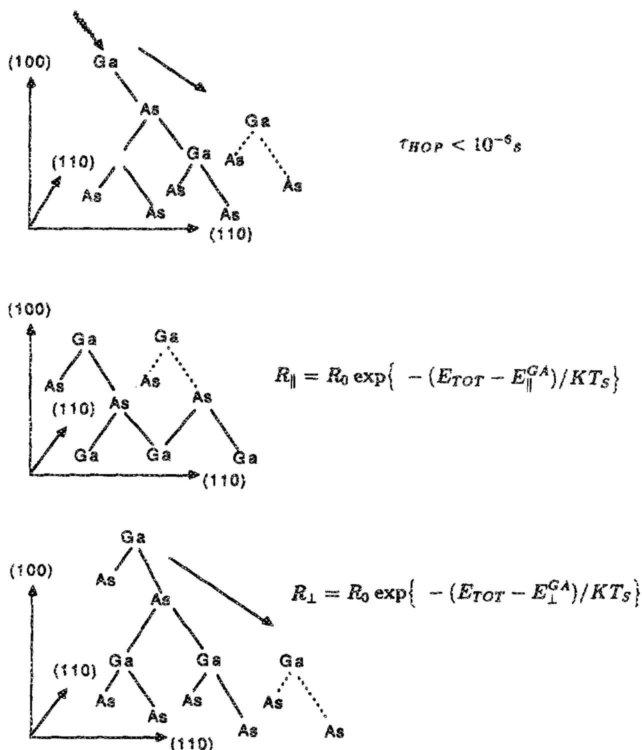

FIG. 2. Cation migration processes on growing surface during growth of GaAs by molecular-beam epitaxy.

B. The metal growth

Some of the issues in metal growth related to surface kinetics have been discussed above. Another important issue is that of lattice mismatch. While the Al and GaAs have an underlying FCC structure, the lattice constant differs by $\sim 14\%$. The situation is far better for (110) Al [on (100) GaAs] where the difference is reduced to $\approx 1.4\%$. However, the x-ray results discussed below reveal that the metal grows in a (111) orientation. This is favored energetically by the close packing of atoms. The growth must occur at low temperatures due to the weaker Al—Al bonds (compared to the Ga—As bond). At higher temperatures, thermodynamic considerations suggest that one may have entropy-controlled growth and thus have a rough growth front.

The real problem in buried metal growth occurs when the semiconductor is grown on the Al film. Since the Al—As bond is much stronger than the Al—Al bond, as soon as the As_4 flux is turned on, the metal layer will tend to form AlAs. The only possibility of stopping this is to limit this reaction through kinetic barriers. Low-temperature growth provides one such barrier. However, for reasons discussed previously, one can grow high-quality semiconductors at low temperatures only by MEE techniques. Our results discussed in the experimental section clearly show the effects on lowering the growth temperature on the nature of the Al film. Use of Ni, as done by Harbison and co-workers[3,4] possibly also provides a similar kinetic barrier.

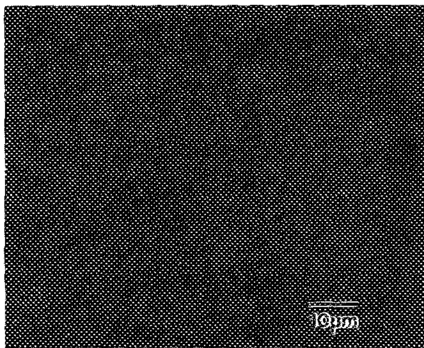

FIG. 3. Surface morphology of a 0.5-μm GaAs superlayer grown by MEE on Al at 400 °C.

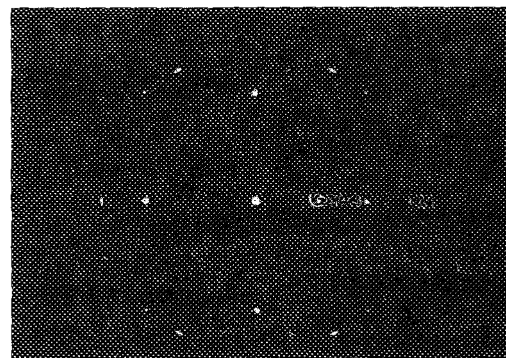

a

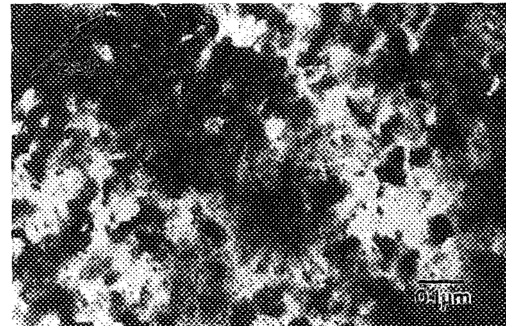

b

FIG. 4. (a) Transmission electron diffraction pattern and (b) dark-field image micrograph of 200-Å Al film deposited on GaAs by MBE at 0 °C at a rate of 1 μm/h.

III. EPITAXIAL GROWTH

A series of GaAs/Al/GaAs heterostructures were grown by a combination of MBE and MEE. A typical structure grown on an indium-mounted (100) GaAs substrate is as follows. Ten periods of a GaAs(41 Å)/ $Al_{0.3}Ga_{0.7}As$ (40 Å) superlattice followed by a 0.5-μm undoped GaAs buffer are first grown by MBE at 600 °C at a rate of 1 μm/h. The As_4 flux is then turned off so that the background pressures falls to $\sim 10^{-9}$ Torr. At the same time the substrate heater is turned off and the substrate is made to face the cryoshroud walls so that the substrate temperature is slowly lowered to ~0 °C. 100–400 Å of Al is then grown at a rate of ~0.2 μm/h. The As flux is then increased to $\sim 10^{-5}$ torr, with the substrate still facing the cryoshrouds. The substrate is then heated to the growth temperature of the GaAs superlayer. This layer (usually 0.3 μm thick) is grown by MEE at 200 or 400 °C by alternate impingement of Ga (at which time $P_{As_4} \sim 10^{-6}$ Torr) and As fluxes ($P_{As_4} \sim 10^{-5}$ Torr) with a growth rate of one monolayer every 2 s.

Growth of the heterostructure was monitored by *in situ* RHEED measurements, using a 10-kV electron gun. The usual (2×4) As-stabilized pattern is observed during the growth of the GaAs buffer layer. At the initiation of Al growth, the pattern is spotty, but becomes streaked with a wider spacing after ten monolayers are grown. This pattern is maintained until Al growth is terminated. It was observed that for GaAs superlayer growth with $T_{sub} > 300$ °C under an As overpressure (As shutter closed), the spacing between the streaks decreased to that seen for GaAs. At lower substrate temperatures this was not observed. We therefore believe that when the growth of the superlayer GaAs is resumed at 200 °C, there is no severe reaction of Al with residual As to form AlAs. After growth of ~500 Å of GaAs, a clear (2×4) reconstruction pattern was seen for growth at 200 and 400 °C. The surface morphology of the top layer, as seen by Nomarski interference contrast is depicted in Fig. 3. Visually, the surface appears to be smooth for growth at 400 °C, but seems to have a slight haze for growth at 200 °C.

The crystallinity and orientation of an Al thin film was studied by growing a single Al film on GaAs substrate. After a 0.3-μm GaAs buffer was grown at 600 °C, the As source temperature and the substrate temperature were slowly reduced. The As shutter was closed when the substrate temperature reached 400 °C. At 200-Å Al thin film was then deposited on the (001) GaAs substrate with a growth rate of 1.0 μm/h at 0 °C. This thin film was studied by transmission electron diffraction and dark-field imaging using the Al reflections. The diffraction pattern and the micrograph are shown in Figs. 4(a) and 4(b), respectively. Examining Fig. 4(a), it is found that in addition to GaAs (001) diffraction spots, there are textured Al reflections. Double diffraction is also clearly seen in the diffraction pattern. The texture is localized around reflections of [111] axes, and this shows that the film is polycrystalline with preferred directions distributed. The minimum energy configuration of a crystal lattice is at the close-packed plane, which is in the (111) directions for the face-centered Al cubic lattice. The Al thin film deposited at 0 °C, with very low surface diffusivity, is hence favored to nucleate along the (111) orientations. The orientation relationships between Al and GaAs are Al[111]//GaAs[001] and Al[200]//GaAs[220]. The Al[220] dark-field micrograph shown in Fig. 4(b) reveals the polycrystalline morphology. A large number of Moiré fringes are also observed in the micrograph. It should be noted that Petroff *et al.*[7] observed (110)- and (100)-oriented Al films or completely (100)-oriented Al films deposited on GaAs at room temperature

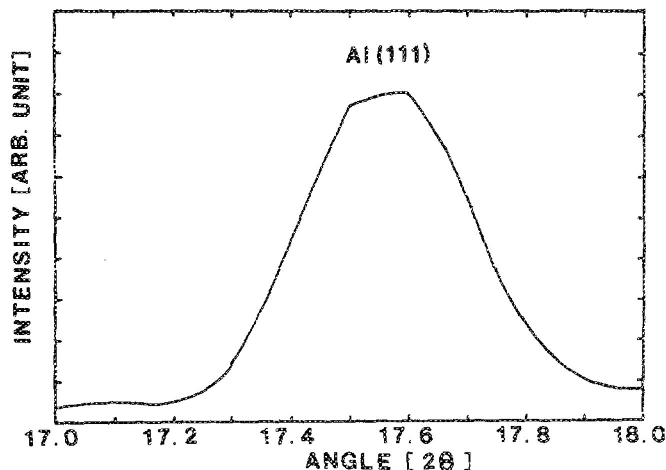

FIG. 5. X-ray diffraction scan of Al/GaAs heterostructure. The Al peak corresponds to a (111) orientation.

(~20 °C), and (110) growth of Al on (100) GaAs has also been reported by Ludeke, Chang, and Esaki.[8] It is apparent that the nucleation mechanism may be quite different for different deposition temperatures.

The confirmation of the preferred (111) orientation of the polycrystalline grains comes from x-ray diffraction measurements done by the four-circle method. The scan was run over GaAs (400), and Fig. 5 shows a diffracted signal from Al corresponding to a (111) orientation. The linewidth is broad (0.35°), which corresponds to a coherence length of ~60 Å for the Al grains. It may therefore be concluded that the Al growth is in the (111) direction.

IV. CHARACTERIZATION OF BURIED METAL HETEROSTRUCTURES: RESULTS AND DISCUSSION

A. Transmission electron microscopy

Cross-sectional transmission electron microscopy (TEM) measurements were made on the different samples to evaluate the growth modes and structural integrity of the buried metal layers. The micrographs of structures grown by MEE at 200 and 400 °C are shown in Figs. 6(a) an 6(b), respectively. While there is considerable outdiffusion and balling of the Al in the latter case, very little or no such outdiffusion is noticed in the former. The top GaAs layer grown at 200 °C also shows a considerable amount of twinning, which has also been observed in the case of NiAl-GaAs.[3]

B. Secondary-ion mass spectroscopy (SIMS)

The depth profiles of the different atomic species were obtained by secondary-ion mass spectroscopy, using Cs ions, at Charles Evans and Associates. The results are shown in Fig. 7 for a structure in which the top GaAs layer was grown by MEE at 200 °C. The nominal Al thickness is 200 Å. For comparison, the Al (100 Å) profile for a structure in which the top layer is grown by MEE at 400 °C is also shown by dotted lines. It is clear that, while the Al peak remains very sharp and symmetrical for MEE growth

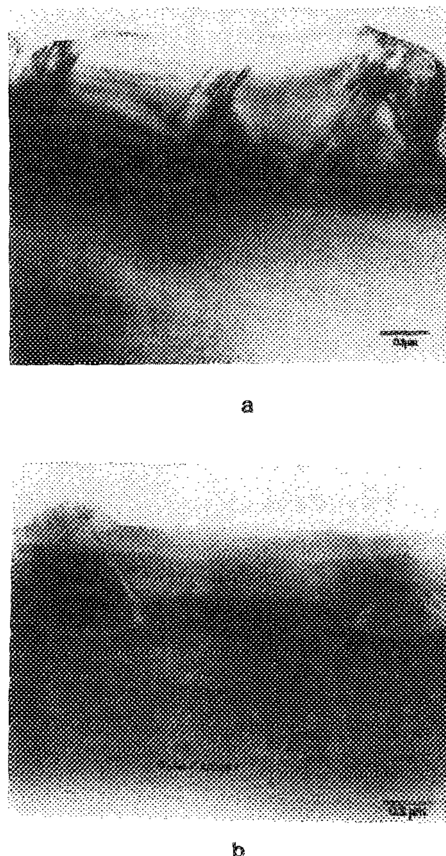

FIG. 6. Cross-sectional transmission electron micrograph of GaAs/Al/GaAs heterostructures with the GaAs superlayer grown by MEE at (a) 200 °C and (b) 400 °C.

at 200 °C, the one grown at 400 °C is broad and asymmetrical. In the case of a structure in which 100-Å Al was deposited and the top GaAs was grown at 400 °C by MBE at 1 μm/h, the broadening of the Al peak was far less. This

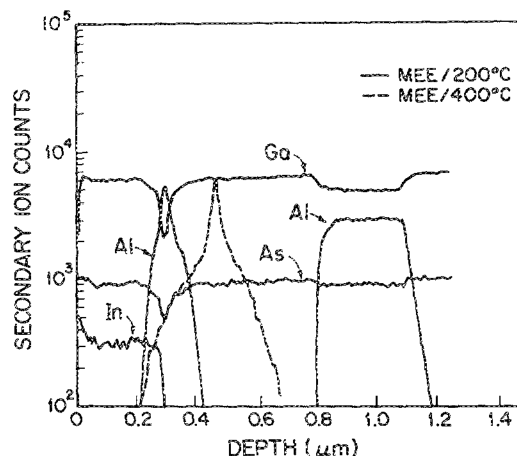

FIG. 7. SIMS profile of the GaAs/Al/GaAs structure with the GaAs top layer grown by MEE at 200 °C. The thickness of the Al film is estimated to be 100 Å. The dashed line indicates the Al profile for a sample in which the Al film thickness is 100 Å, and the top layer is grown at 400 °C.

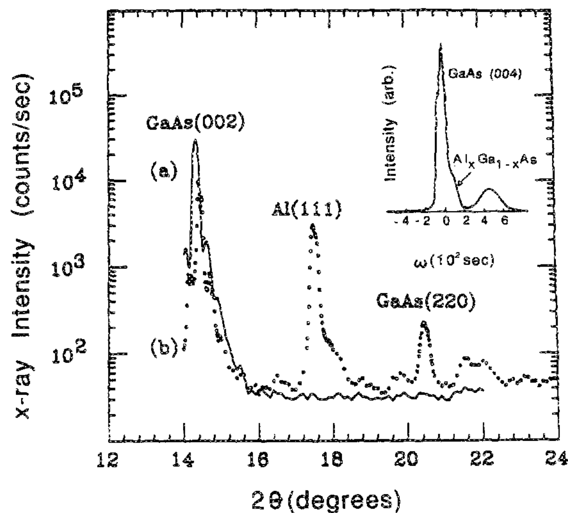

FIG. 8. X-ray diffraction scans of GaAs/Al/GaAs heterostructures with top layer grown at (a) 400 °C (solid line) and (b) 200 °C (dots). Features in the vicinity of (002) are due to the buffer superlattice. The inset shows rocking curve of the 400 °C sample showing the presence of $Al_xGa_{1-x}As$ ($x \approx 0.08$). The peak at $\omega \approx 500$ s is due to In doping of the top GaAs layer.

is understandable, since the total growth time of the superlayer is reduced by a factor of 2. Therefore, the temperature and time of growth are extremely critical in controlling the integrity of the buried Al layer.

C. X-ray diffraction

X-ray diffraction data on the GaAs-Al-GaAs structure are shown in Fig. 8. We employed a combination of techniques including four-circle diffractometry and double-crystal rocking curve analysis. The former method gives overall information on the degree of perfection of the layers, their stacking and orientation, while the double-crystal technique is capable of a very high-resolution determination of chemical composition variations and the resulting strains. The data in Fig. 8 are for a diffraction vector normal to the (100) substrate surface. Immediately, it is clear that the sample with the top layer grown at 400 °C is of higher structural quality than the 200 °C structure. In particular, the presence of a significant (220) GaAs peak in the latter sample is evidence that twinning occurs in the regrowth of GaAs on top of the Al layer, which we find to be in the (111) close-packed orientation. The 110-twinned regions are found to have very broad rocking curve widths ($\approx 5°$ FWHM), indicating poor alignment with the substrate; this is probably a consequence of the lattice mismatch introduced by the (111) Al layer. In contrast, the sample grown at higher temperature shows no evidence of twinning; however, there is no x-ray peak from Al in this sample, suggesting that alloying has taken place. Our double-crystal results in the inset confirm that this is indeed the case.

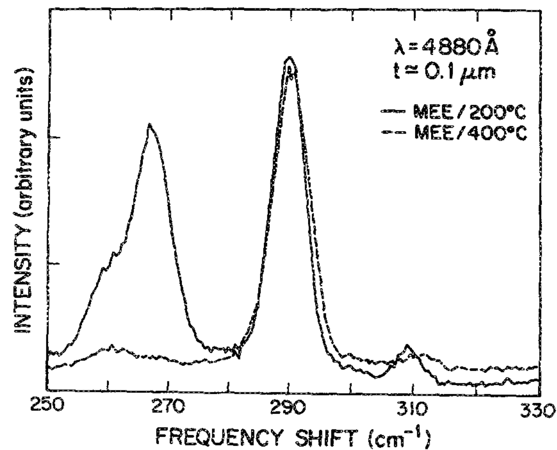

FIG. 9. Raman spectra of GaAs/Al/GaAs structure, with the top layer grown at 200 °C, showing phonon scattering. The dashed profile is for the top layer grown at 400 °C.

D. Raman spectroscopy

The Raman spectrum of the 200 and 400 °C grown structures at $T = 300$ K are shown in Fig. 9. The data were obtained using the 4880-Å line of an Ar^+ laser in a nearly backscattering configuration. The notation $z(x', x')\bar{z}$ indicates that the incident (scattered) photon propagates along $z = [100]$ ($\bar{z} = [\bar{1}00]$) with polarization $x' = [011]$. Here the directions refer to the crystal axes of the substrate. Our data on the 200 °C sample show no evidence of alloying effects. The spectral features of 267 and 290 cm^{-1} are due to the bulk transverse (TO) and longitudinal-optical (LO) phonons of the top GaAs layer (the penetration depth of the light is approximately 0.1 μm). These lines appear in the geometry $z(x',x')\bar{z}$ ($y \approx [1\bar{1}1]$). In III-V compounds, backscattering from (100) surfaces allows only the LO mode, while for (110) only the TO phonon is allowed. Therefore, the observation of both TO and LO peaks is consistent with the x-ray findings showing both (100) and (110) orientations for the top layer. Moreover, the observed selection rules indicate that the GaAs substrate and the top layer share a common [110] axis. Other than the two optical modes, the spectrum shows weaker features at 260 and 310 cm^{-1}. Unlike the TO and LO phonons, these peaks also appear in the $z(x',y')\bar{z}$ configuration, and furthermore, their intensity and line shape depend on the angle between the directions of the incident and scattered beams. This and the positions of the peaks suggest that they are due to bulk polaritons; however, such excitations are nominally forbidden in backscattering. The structure for which the top GaAs layer was grown at 400 °C also shows the extra lines in the Raman spectrum, but no TO mode. The latter fact indicates that the top layer orientation is (110), in agreement with the x-ray results.

E. Low-temperature photoluminescence measurements

As mentioned earlier, the optical quality of the superlayer is of tremendous importance for the design and realization of optoelectronic devices. With that in mind we

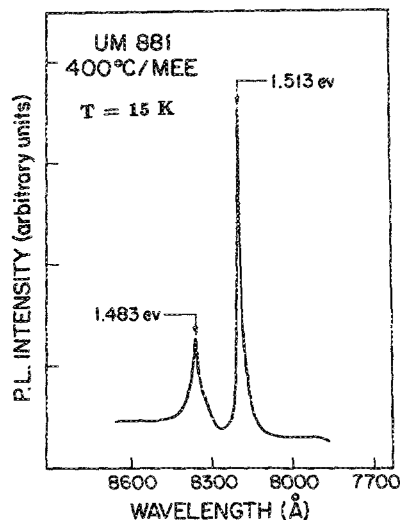

FIG. 10. Low-temperature photoluminescence spectrum from the top GaAs grown at 400 °C in a GaAs/Al/GaAs structure.

have measured the low-temperature photoluminescence of the superlayers grown by MEE. Excitation was provided by the 5145-Å line of an Ar^+ laser, and the luminescence was analyzed and detected by a 1-m Jarell-Ash scanning spectrometer and a S1 photomultiplier tube, respectively. Figure 10 shows the 15-K photoluminescence spectrum of a sample in which the 0.4-μm GaAs superlayer was grown by MEE at 400 °C. The layer was alloyed with a small amount of In (~1%). The peak at 1.513 eV probably corresponds to a donor-bound excitonic transition, and the peak at 1.483 eV appears to be related to carbon acceptors (free-to-bound transition). Carbon incorporation is usually higher in layers grown by MEE than in those grown by MBE. In contrast, no photoluminescence was observed from the superlayers grown by MEE at 200 °C.

It is apparent from the results described above that low-temperature growth of the superlayer is essential for the integrity of the metal-semiconductor heterointerface. The use of MEE allows the growth temperature to be lowered considerably. However, it is seen that at a growth temperature of 200 °C, where the buried Al layer has good structural integrity, the superlayer shows extensive twinning and no luminescence is detected from it. Therefore, this temperature may be too low for growing device-quality GaAs. It would therefore be useful to investigate the growth of other semiconductors, which have lower ideal growth temperatures under normal MBE conditions, such as $In_{0.53}Ga_{0.47}As/InP$. We have recently grown high-quality InGaAs at temperatures as low as 350 °C, and this growth temperature can be further lowered by using MEE. Moreover, InGaAs, InGaAs/InAlAs, and InGaAs/InP lattice matched to InP are important materials and heterostructures for fiber-optical communication.

V. CONCLUSION

In our study reported here we have demonstrated that MEE is a viable technique for growing semiconductor/metal heterostructures. GaAs/Al/GaAs heterostructures with the superlayer grown by MEE at 200 °C seems to preserve the structural quality of the buried Al layer. However, there is considerable twinning in this superlayer, and no luminescence is observed even at low temperatures. On (100) GaAs the Al layer grows polycrystalline with the preferred orientation in each grain being (111). The top GaAs layer, which is twinned, consists of a mixture of (100) and (110) orientations. Overall, the structural character of the samples is determined by a complex balance between interdiffusion, alloy formation, and the kinetics of metal-semiconductor epitaxy.

ACKNOWLEDGMENTS

The work was supported by the National Science Foundation (MRG Program) under Grant DMR-8602675, the Army Research Office (URI Program) under Contract DAAL-03-87-K0007, and the Department of Energy under Grant DE-FG02-86ER45250.

[1] T. Sands, Appl. Phys. Lett. 52, 197 (1988).
[2] T. Sands, V. G. Keramidas, J. Washburn, and R. Gronsky, Appl. Phys. Lett. 48, 402 (1986).
[3] T. Sands, J. P. Harbison, W. K. Chan, S. A. Schwarz, C. C. Chang, C. J. Palmstrom, and V. G. Keramidas, Appl. Phys. Lett. 52, 1216 (1988).
[4] J. P. Harbison, T. Sands, N. Tabatabaie, W. K. Chan, L. T. Florez, and V. G. Keramidas, Appl. Phys. Lett. 53, 1717 (1988).
[5] Y. Horikoshi, M. Kawashime, and H. Yamaguchi, Jpn. J. Appl. Phys. 25, L868 (1986).
[6] B. Tadayon, S. Tadayon, M. G. Spencer, G. L. Harris, L. Rathbun, J. T. Bradshaw, W. J. Schaff, P. J. Tasker, and L. F. Eastman, Appl. Phys. Lett. 53, 2664 (1988).
[7] P. M. Petroff, L. C. Feldman, A. Y. Cho, and R. S. Williams, J. Appl. Phys. 52, 7317 (1981).
[8] R. Ludeke, L. L. Chang, and L. Esaki, Appl. Phys. Lett. 23, 202 (1973).